Les Cahiers du GERAD ISSN: 0711–2440

Numerical certification of Pareto optimality for biobjective nonlinear problems

C. Audet,
F. Messine, J. Ninin

G–2020–01

January 2020

La publication de ces rapports de recherche est rendue possible grâce au soutien de HEC Montréal, Polytechnique Montréal, Université McGill, Université du Québec à Montréal, ainsi que du Fonds de recherche du Québec – Nature et technologies.

Dépôt légal – Bibliothèque et Archives nationales du Québec, 2020
– Bibliothèque et Archives Canada, 2020

The publication of these research reports is made possible thanks to the support of HEC Montréal, Polytechnique Montréal, McGill University, Université du Québec à Montréal, as well as the Fonds de recherche du Québec – Nature et technologies.

Legal deposit – Bibliothèque et Archives nationales du Québec, 2020
– Library and Archives Canada, 2020

GERAD HEC Montréal
3000, chemin de la Côte-Sainte-Catherine
Montréal (Québec) Canada H3T 2A7

Tél. : 514 340-6053
Téléc. : 514 340-5665
info@gerad.ca
www.gerad.ca

Numerical certification of Pareto optimality for biobjective nonlinear problems

Charles Audet [a,b]
Frédéric Messine [c]
Jordan Ninin [a,d]

[a] *GERAD, HEC Montréal, Montréal (Québec), Canada*

[b] *Department of Mathematics and Industrial Engineering, Polytechnique Montréal (Québec) Canada*

[c] *University of Toulouse, ENSEEIHT-LAPLACE, Toulouse, France*

[d] *ENSTA-Bretagne, Lab-STICC, team PRASYS, Brest, France*

charles.audet@gerad.ca
jordan.ninin@ensta-bretagne.fr

January 2020
Les Cahiers du GERAD
G–2020–01

Abstract: The solution to a biobjective optimization problem is composed of a collection of trade-off solution called the Pareto set. The present work studies the question of certifying numerically that a conjectured set is close to the Pareto set. Two situations are considered. First, we analyze the case where the conjectured set is directly provided: one objective is explicitly given as a function of the other. Second, we analyze the situation where the conjectured set is parameterized: both objectives are explicitly given as functions of a parameter. In both cases, we formulate the question of verifying that the conjectured set is close to the Pareto set as a global optimization problem. These situations are illustrated on a new class of extremal problems over convex polygons in the plane. The objectives are to maximize the area and perimeter of a polygon with a fixed diameter, for a given number of sides.

Keywords: Biobjective optimization, numerical certification, polygon, perimeter, area, diameter

Acknowledgments: Work of the first author was supported by NSERC grant 239436–01.

1 Introduction

In many situations, more than one objective need to be considered by an optimization problem. The present work focuses on biobjective optimization problems of the form

$$\max_{x\in\Omega} \quad (f_1(x), f_2(x)) \tag{1}$$

where $\Omega \subset \mathbb{R}^n$ is a closed set, and $f_i : \Omega \to \mathbb{R}$ are real-valued functions, for $i \in \{1, 2\}$. In general, there is no single vector $x \in \Omega$ that simultaneously maximizes both objectives. The solution of the biobjective problem consists of the set of tradeoff points selected according to the Pareto dominance relation [38] which compares two different decision vectors $u \in \Omega$ and $v \in \Omega$. In a maximization context, the vector $u \in \Omega$ is said to dominate $v \in \Omega$ (denoted $u \succ v$) if both objective function values evaluated at u are greater than or equal to those evaluated at v with at least one strict inequality.

The set of nondominated points defines the solution set of the biobjective problem. Pareto optimality is formally defined in Definition 1

Definition 1 *A point $v \in \Omega$ is said to be* Pareto optimal *if and only if there is no $u \in \Omega$ such that $u \succ v$. The set of all Pareto optimal points is called the* Pareto set*, and its image in $\mathbb{R}^2$ is called the* Pareto front*, denoted by $\mathcal{P}$.*

In the biobjective case, the Pareto set satisfies an ordering property: any two Pareto optimal points $u \in \Omega$ and $v \in \Omega$ satisfy $f_1(u) > f_1(v)$ if and only if $f_2(u) < f_2(v)$. This ordering property is lost when the optimization problem contains more than two objectives.

The present paper is not about devising a method to generate the Pareto front. The interested reader may consult one of the recent surveys [3, 20, 21, 34, 39] on multiobjective optimization, including methods to approximate and compare Pareto fronts. Our work is not as general, and considers situations in which one has what he believes to be the Pareto front, and wishes to certify numerically that it is true. This task is similar to providing a certificate of global optimality of a single solution in mono-objective optimization, with the important difference that an entire set of solutions needs to be validated.

Let $\tilde{\mathcal{P}} \subset \mathbb{R}^2$ denote our conjectured approximation of the Pareto front $\mathcal{P}$. Two types of situations are considered. First, we propose a strategy where an analytical formulation of $\tilde{\mathcal{P}}$ explicitly gives one of the objectives as a function of the other. Second, we consider the case where both objectives are parameterized by a single variable on a known interval. In both situations, we propose a generic way to numerically certify that $\tilde{\mathcal{P}}$ is close to the Pareto front $\mathcal{P}$.

Our methodology is then applied to a new class of optimization problems from planar geometry. We study the optimal tradeoffs between maximal perimeter and maximal area of unit-diameter polygons and give numerical results for the hexagon that illustrate the strategies describing $\tilde{\mathcal{P}}$.

The structure of the paper is as follows. Section 2 describes two strategies to certify a given approximation $\tilde{\mathcal{P}}$ of the Pareto front $\mathcal{P}$ of a biobjective problem. Section 3 details two optimization problems from planar geometry, and provides a conjectured approximation $\tilde{\mathcal{P}}$ of their Pareto front. Extensive numerical experiments are reported in Section 4. For the second problem, the Pareto front is discontinuous and each connected part is treated separately. Finally, the last section contains some concluding remarks.

2 Pareto front certification

In mono-objective numerical global optimization, numerical certification of a candidate solution is usually accompanied by a small tolerance parameter denoted by a scalar $\varepsilon > 0$. We use the following definition in the context of a biobjective optimization problem.

Definition 2 *Let $\varepsilon > 0$ be a fixed scalar and $\tilde{\mathcal{P}}_I \subset \mathbb{R}^2$ be a curve whose projection on the abscissa is a nonempty interval denoted I. The set $\tilde{\mathcal{P}}_I$ is said to be a* ε-Pareto approximation of the Pareto front $\mathcal{P}$ on the interval I *if for every $(a, b) \in \tilde{\mathcal{P}}_I$ there exists an $u \in \Omega$ such that $a = f_1(u)$ and $b = f_2(u)$, and in addition, there are no $v \in \Omega$ such that $f_1(v) \geq a + \varepsilon$ and $f_2(v) \geq b + \epsilon$.*

The entire Pareto front is not necessarily connected, and may sometimes be obtained by the union of connected parts (as illustrated by the last example in Section 4.3). We consider problems in which the Pareto front is composed of m parts:

$$\mathcal{P} = \bigcup_{i=1}^{m} \mathcal{P}_{I_i}$$

where $\{I_i\}_{i=1}^m$ are disjoint intervals.

Definition 3 *Let $\varepsilon > 0$ be a fixed scalar and for each $i \in \{1, 2, \ldots, m\}$ let $\tilde{\mathcal{P}}_{I_i} \subset \mathbb{R}^2$ be a ε-Pareto approximation of the Pareto front component $\mathcal{P}_{I_i}$. Then*

$$\tilde{\mathcal{P}} = \bigcup_{i=1}^{m} \tilde{\mathcal{P}}_{I_i}$$

is said to be ε-Pareto approximation of the Pareto front $\mathcal{P}$.

2.1 Certification of a connected part of an analytical front

The first situation that we consider is when one has a conjecture that provides an analytical direct representation of one of the objective function in terms of the other on the Pareto front. More precisely, let $I \subset \mathbb{R}$ be an interval on the value of the first objective function value (for conciseness we use I rather than I_i for some $i \in \{1, 2, \ldots, m\}$), and let $g : I \to \mathbb{R}$ be a function such that the set

$$\tilde{\mathcal{P}}_I = \left\{(a, g(a)) \in \mathbb{R}^2 \ : \ a \in I\right\}$$

is believed to be the part of the Pareto front $\mathcal{P}$ where the values of the first objective function are taken from I.

Proposition 1 *Suppose that for each $a \in I$, there exists an $u \in \Omega$ such that $f_1(u) = a$ and $f_2(u) = g(a)$. Then $\tilde{\mathcal{P}}_I$ is equal to the Pareto front component $\mathcal{P}_I$ if and only if the optimal value of the mono-objective problem*

$$\begin{array}{ll} \max\limits_{x \in \Omega} & f_2(x) - g(f_1(x)) \\ s.t. & f_1(x) \in I \end{array} \tag{2}$$

is zero.

Proof. Consider any $(a, b) \in \tilde{\mathcal{P}}_I$. By definition $b = g(a)$ and $a \in I$, and by the assumption, there exists an $u \in \Omega$ such that $f_1(u) = a \in I$ and $f_2(u) = g(a)$. Therefore u satisfies the constraints of Problem (2) and the optimal value is nonnegative since $f_2(u) - g(f_1(u)) = 0$.

If the optimal value of Problem (2) is zero, then $f_2(x) \leq g(f_1(x))$ for all $x \in \Omega$ with $f_1(x) \in I$ and consequently $\tilde{\mathcal{P}}_I \subseteq \mathcal{P}_I$.

If the optimal value of Problem (2) is strictly positive, then there exists an optimal solution x of (2) such that $f_2(x) > g(f_1(x))$ which implies that $(f_1(x), f_2(x)) \in \tilde{\mathcal{P}}_I$ but $(f_1(x), f_2(x))$ is not a Pareto front point. □

In the situation where $\tilde{\mathcal{P}}_I$ is a subset of the Pareto front, solving Problem (2) causes some numerical difficulties because every Pareto point is a global optimal solution of the problem. So in practice, we introduce a small scalar $\varepsilon > 0$ and add an additional constraint that makes the domain void when $\tilde{\mathcal{P}}_I$ is a subset of the Pareto front:

$$\begin{array}{ll} \max\limits_{x\in\Omega} & f_2(x) - g(f_1(x)) \\ \text{s.t.} & f_2(x) - g(f_1(x)) \geq \varepsilon \\ & f_1(x) \in I. \end{array} \tag{3}$$

The goal is now to apply a global optimization algorithm to this problem to show that there are no feasible solutions. If there are no feasible solutions to Problem (3), and if for each $a \in I$, there exists an $u \in \Omega$ such that $f_1(u) = a$ and $f_2(u) = g(a)$, then $\tilde{\mathcal{P}}_I$ is an ε-Pareto approximation of $\mathcal{P}$ on I, in the sense of Definition 3. Alternately, if the global optimization algorithm finds an optimal solution to this problem, then this solution belongs to the Pareto set, showing that the conjectured set is incorrect.

2.2 Certification of a connected part of a parameterized front

The second situation is when one has a conjecture that provides a parameterized representation of both objective functions on the Pareto front. More precisely, for $i \in \{1, 2\}$ let $g_i : [\underline{q}, \overline{q}] \to \mathbb{R}$ be functions defined on an interval delimited by the scalars $\underline{q}, \overline{q} \in \mathbb{R}$. The conjectured Pareto front on the interval $I = [g_1(\underline{q}), g_1(\overline{q})]$ is

$$\tilde{\mathcal{P}}_I = \left\{(a, b) \in \mathbb{R}^2 \ : \ a = g_1(q),\ b = g_2(q),\ q \in [\underline{q}, \overline{q}]\right\}.$$

Proposition 2 *Suppose that for any $(a, b) \in \tilde{\mathcal{P}}_I$, there exists an $u \in \Omega$ and a scalar $q \in [\underline{q}, \overline{q}]$ such that $f_1(u) = g_1(q) = a$ and $f_2(u) = g_2(q)$. Then $\tilde{\mathcal{P}}_I$ equals the Pareto front component $\mathcal{P}_I$ if and only if the optimal value of the problem*

$$\begin{array}{ll} \max\limits_{x\in\Omega, q\in\mathbb{R}} & f_2(x) - g_2(q) \\ s.t. & f_1(x) \geq g_1(q) \\ & q \in [\underline{q}, \overline{q}] \end{array} \tag{4}$$

is zero.

Proof. Consider any $(a, b) \in \tilde{\mathcal{P}}_I$. By definition $a = g_1(q), b = g_2(q)$ for some $q \in [\underline{q}, \overline{q}]$, and by the assumption, there exists an $u \in \Omega$ such that $f_1(u) = g_1(q) = a$ and $f_2(u) = g_2(q)$. Therefore a satisfies the constraints of Problem (2) and the optimal value is nonnegative.

If the optimal value of Problem (4) is zero, then $f_2(x) \leq g_2(q)$ for all $x \in \Omega$ and $q \in [\underline{q}, \overline{q}]$ with $f_1(x) \geq g_1(q)$ and consequently $\tilde{\mathcal{P}}_I \subseteq \mathcal{P}_I$.

If the optimal value of Problem (4) is strictly positive, then there exists an optimal solution $x \in \Omega$ and $q \in [\underline{q}, \overline{q}]$ such that $f_2(x) > g(q)$ and $f_1(x) \geq g_1(q)$. It follows that $(a, b) := (g_1(q), g_2(q))$ belongs to $\tilde{\mathcal{P}}_I$ but not to the Pareto front $\mathcal{P}_I$. □

As in the previous subsection, solving this problem is subject to numerical difficulties. So we introduce a second feasibility problem for a fixed scalar $\varepsilon > 0$

$$\begin{array}{lll} \max\limits_{x\in\Omega, q\in\mathbb{R}} & f_2(x) - g_2(q) & \\ \text{s.t.} & f_i(x) - g_i(q) \geq \varepsilon & i \in \{1, 2\} \\ & q \in [\underline{q}, \overline{q}]. & \end{array} \tag{5}$$

Again, if there are no feasible solutions to Problem (5), and if for each $a \in I$, there exists an $u \in \Omega$ and a scalar $q \in [\underline{q}, \overline{q}]$ such that $f_1(u) = g_1(q) = a$ and $f_2(u) = g_2(q)$, then $\tilde{\mathcal{P}}_I$ is an ε-Pareto approximation of $\mathcal{P}$ on I, in the sense of Definition 3.

3 Maximizing the area and perimeter of small hexagons

A number of authors studied the questions of maximizing an attribute such as area, perimeter, diameter, width and sum of distances between vertices of a n-sided planar convex polygon, while fixing another attribute to a fixed value. Surveys of recent progress on these problems can be found in [1, 4, 6].

These problems can be generalized, by optimizing over more than one attribute. We consider in the remaining of the paper the biobjective problem of maximizing the area and perimeter of unit-diameter convex polygons. Recall that the diameter of a polygon is defined to be the length of the longest line segment joining two of its vertices.

3.1 Optimization problems in planar geometry

Throughout the paper we use the following notation. For a given value of n, let Ω denote the set of convex n-sided polygons with diameter equal to 1; such polygons are said to be *small*. For any polygon $x \in \Omega$, let P and A denote the perimeter and area. The biobjective problem considered in the present work may be stated as

$$\max_{x \in \Omega} \quad (P,\ A)\,. \tag{6}$$

The cases where the number of sides is odd is trivial, since Reinhardt [32] and Tamvakis [35] show that the regular polygons are optimal for both single-objective optimization problems. It follows that the set of Pareto optimal solution is a singleton.

We consider two families of problems. First, we study equilateral polygons. For any value of $n \geq 3$, the small n-gon that maximizes the area is the regular n-gon [2]. However, when $n \geq 8$ is a power of two, the small equilateral polygon that maximizes the perimeter is not the regular polygon [7]. When $n \geq 3$ is not a power of two, the optimal solutions which maximize the perimeter are clipped-Reuleaux polygons [35, 37].

Second, we study polygons that are not constrained to be equilateral. The cases where the number of sides n is even is not trivial. For the maximization of the area, Foster and Szabo [12] prove a conjecture of Graham [14] stating that the optimal diameter graph consists of a cycle of length $n-1$ together with a pending edge. This additional structure allows Henrion and Messine [16] to numerically certify cases up to $n = 10$ in a few minutes using a semi-definite global optimization approach. The exact solution for the hexagon is shown to be the root of a degree 10 polynomial with integer coefficients [14], and under an axial symmetry assumption, the exact solution for the octagon is shown to be the root of a degree 42 polynomial with integer coefficients [9]. Mossinghoff [29] constructs families of approximate solutions with a guarantee that the error is less than $O(\frac{1}{n^3})$. For the maximization of the perimeter, the optimal solutions are equilateral polygons clipped-Reuleaux polygons when n is not a power of two [35]. The maximization of the area and perimeter of the octagon are studied in [5, 8, 13].

The quadrilateral case is easy. It can easily be shown that the square is the small equilateral quadrilateral that maximizes both the perimeter $P = 2\sqrt{2}$ and area $A = \frac{1}{2}$. In the non-equilateral case, any small quadrilateral with two perpendicular unit diagonals maximizes the area. The Tamvakis quadrilateral [35] maximizes the perimeter, and has two perpendicular unit diagonals. Therefore, the Pareto front for the quadrilateral contains a single solution with a perimeter $P = 2 + 2\sqrt{2 - \sqrt{3}}$ and area $A = \frac{1}{2}$.

The remaining of the section is devoted to the next case: the hexagon.

3.2 The equilateral hexagon

This section is devoted to equilateral small hexagons. The regular hexagon maximizes the area, and the clipped-Reuleaux hexagon maximizes the perimeter. Table 2 gives lower and upper bounds on the Pareto front.

Table 1: Bounds on the perimeter and area of Pareto equilateral small hexagons

	Perimeter		Area	
regular	$\underline{p} =$	3	$\overline{a} = \frac{3\sqrt{3}}{8} \approx$	0.6495190530
clipped-Reuleaux	$\overline{p} = 6\sqrt{2-\sqrt{3}} \approx$	3.105828541	$\underline{a} = \frac{1}{2}(3-\sqrt{3}) \approx$	0.6339745960

In order to conjecture about the nature of the Pareto front, we consider an equilateral triangle with side length s and add a vertex at unit distance from each of the vertices of the triangle by bisecting each angle. Figure 1 illustrates the resulting hexagon.

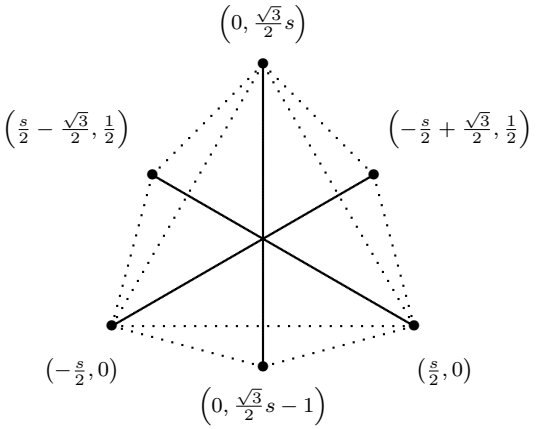

Figure 1: An equilateral triangle with side length s, with three pending diameters forming a small equilateral hexagon

The perimeter P and area A can be written as

$$\begin{aligned} P &= 6\sqrt{\left(\tfrac{\sqrt{3}}{2} - s\right)^2 + \tfrac{1}{4}}, \\ A &= \frac{s}{2}(3 - \sqrt{3}s). \end{aligned}$$

Solving for s in the first equation, and substituting in the second yields the relation between the perimeter and area $A = \frac{\sqrt{3}}{2}\left(1 - \left(\frac{P}{6}\right)^2\right)$ on the interval $I = [\underline{p}, \overline{p}] = [3, 6\sqrt{2-\sqrt{3}}]$. Our conjecture of the Pareto front is the analytical expression

$$\tilde{\mathcal{P}}_I = \left\{ (P, A) \ : \ A = \frac{\sqrt{3}}{2}\left(1 - \left(\frac{P}{6}\right)^2\right), \ P \in I \right\}.$$

We next apply Proposition 1 in which f_1 is the perimeter P, f_2 is the area A, $g(P) = \frac{\sqrt{3}}{2}\left(1 - \left(\frac{P}{6}\right)^2\right)$, $I = [\underline{p}, \overline{p}]$ with the parameterization depicted in Figure 2.

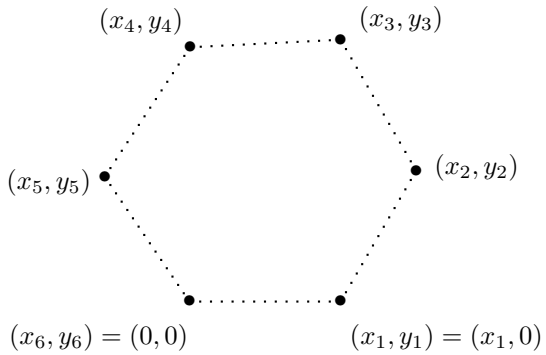

Figure 2: Parameterization of a small equilateral hexagon

The optimization Problem (3) for the equilateral hexagon is therefore

$$
(\mathrm{E}) \left\{ \begin{array}{lll}
\max\limits_{x,y\in\mathbb{R}^6} & \frac{1}{2}\sum\limits_{i=1}^{5}(x_i y_{i+1} - x_{i+1} y_i) - \frac{\sqrt{3}}{2}\left(1 - x_1^2\right) & \\
\text{s.t.} & \frac{1}{2}\sum\limits_{i=1}^{5}(x_i y_{i+1} - x_{i+1} y_i) - \frac{\sqrt{3}}{2}\left(1 - x_1^2\right) \geq \varepsilon & \text{(E0)} \\
& \|(x_{i+1}, y_{i+1}) - (x_i, y_i)\|^2 = x_1^2 \qquad i \in \{1,2,3,4,5\} & \text{(E1)} \\
& \|(x_{i+3}, y_{i+3}) - (x_i, y_i)\|^2 \leq 1 \qquad i \in \{1,2,3\} & \text{(E2)} \\
& \|(x_6, y_6) - (x_4, y_4)\|^2 \leq 1 & \text{(E3)} \\
& \|(x_{i+2}, y_{i+2}) - (x_i, y_i)\|^2 \leq \|(x_6, y_6) - (x_2, y_2)\|^2 \qquad i \in \{1,2,3,4\} & \text{(E4)} \\
& \|(x_5, y_5) - (x_1, y_1)\|^2 \leq \|(x_3, y_3) - (x_1, y_1)\|^2 & \text{(E5)} \\
& -1 \leq x_i \leq 1 \qquad i \in \{2, \cdots, 5\} & \text{(E6)} \\
& 0 \leq y_i \leq 1 \qquad i \in \{2, \cdots, 5\} & \text{(E7)} \\
& x_6 = y_6 = y_1 = 0 & \text{(E8)} \\
& y_2 \geq y_5 & \text{(E9)} \\
& 0.5 \leq x_1 \leq 0.517638090205043 & \text{(E10).}
\end{array} \right.
$$

The constraint (E0) makes the optimization problem infeasible if the conjectured front is indeed the Pareto front. The side lengths are all equal to the variable x_1 and (E1) is the equilateral constraint. (E2–3) are the diameter constraints. (E4) breaks the symmetry by requiring that the longest segment joining two vertices whose indices differ by 2 is associated with the indices 2 and 6 as $(6+2)\text{mod}6 = 2$. (E5) breaks the symmetry by requiring that (x_3, y_3) is further from (x_1, y_1) than (x_5, y_5) is. (E6–7) are trivial bounds that help the numerical optimization procedure. (E8) fixes a vertex at the origin and another on the x axis. This reduces the size of the optimization problem. (E9) breaks vertical symmetry by imposing that the vertex to the right is not lower than the one to the left. (E10) is equivalent to $\underline{p} = 3 \leq P \leq 3.105828541230258 < \overline{p} = 6\sqrt{2-\sqrt{3}}$.

3.3 The hexagon without the equilateral requirement

This section is devoted to small hexagons, that are not restrained to be equilateral. Graham's hexagon [14] maximizes the area. A lower bound on its area is once again achieved by the clipped-Reuleaux hexagon [35] which maximizes the perimeter. Table 2 gives lower and upper bounds on the Pareto front.

Table 2: Bounds on the perimeter and area of small Pareto hexagons

	Perimeter		Area	
Graham	$\underline{p} =$	3.099788706	$\overline{a} =$	0.6749814429
clipped-Reuleaux	$\overline{p} = 6\sqrt{2-\sqrt{3}} \approx$	3.105828541	$\underline{a} = \frac{1}{2}(3-\sqrt{3}) \approx$	0.6339745960

The following lemma provides an upper bound on the side length of a Pareto optimal hexagon. This upper bound is necessary to make the optimization problem tractable.

Lemma 1 *The length of any side of a Pareto optimal hexagon of Problem (6) is less than* 0.978.

Proof. Let c be the length of a side of a Pareto optimal hexagon of Problem (6), and let A denote its area. Figure 3 depicts the region delimited by the two unit-radius circles centered at the vertices of the side of length c, and by the support line containing that side. Let θ be the angle whose cosine is $\frac{c}{2}$. The hexagon is necessarily contained in that region, whose area is $\theta - \frac{1}{2}\sin(2\theta)$.

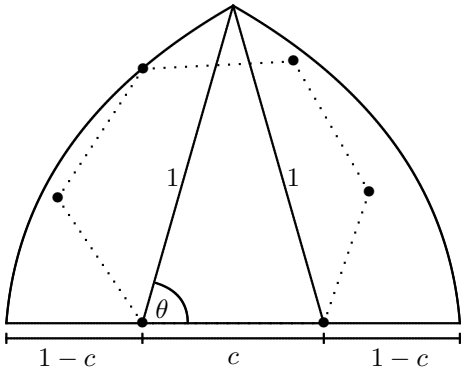

Figure 3: Bounding the side length of a Pareto hexagon

Now, since the area of any Pareto optimal hexagon is bounded below by $\underline{a}$, it follows that

$$\underline{a} \leq A \leq \theta - \frac{1}{2}\sin(2\theta) \quad \Rightarrow \quad \theta > 1.06 \quad \Rightarrow \quad c = 2\cos(\theta) < 0.978.$$

□

Preliminary numerical experiments suggest that the Pareto front is composed of two disjoint parts. Our conjecture is that the diameter graph of the first part is obtained by axially symmetrical hexagons whose diameter graphs are composed of a cycle of length five with a pending diameter, as with Graham's hexagon. This corresponds to the top part of the Pareto front. The second part of the front is conjectured to be generated by axially symmetrical hexagons whose diameter graphs are composed of a path of length four with a pending diameter, as with the clipped-Reuleaux hexagon. This corresponds to the bottom part of the Pareto front. We study both parts independently.

Top part of the Pareto front: A cycle of length five with a pending diameter

Consider an axially symmetrical diameter graph composed of a cycle of length five, together with a pending diameter, and parameterized using the variables u, v and b in $[0, 1]$ as illustrated in Figure 4. The variables defining this hexagon satisfy $u^2 + (b + v)^2 = 1$ and $(u + \frac{1}{2})^2 + v^2 = 1$. By substituting $b = \frac{1}{2}\sqrt{q^2 - 1}$, the perimeter P and area A are parameterized as

$$\begin{aligned} P(q) &= q + \sqrt{6 - \frac{2}{q}\sqrt{q^2-1}\sqrt{16-q^2}} + \sqrt{8 - 2\sqrt{q^2-1} - \frac{2}{q}\sqrt{16-q^2}}, \\ A(q) &= \frac{1}{4}\left(\sqrt{q^2-1} + \frac{1}{q}\sqrt{16-q^2} + \frac{1}{q}\sqrt{q^2-1}\sqrt{16-q^2} - \frac{q}{2}\sqrt{16-q^2} - 1\right). \end{aligned}$$

where the lower bound on q is $\underline{q} = 1.28356703414671$; i.e., $P(\underline{q})$ is equal to the perimeter of Graham's hexagon. The upper bound on q is found by maximizing the function $P(q)$ and corresponds to $\overline{q} = 1.31490238364$ with $P(\overline{q}) = 3.100102486$.

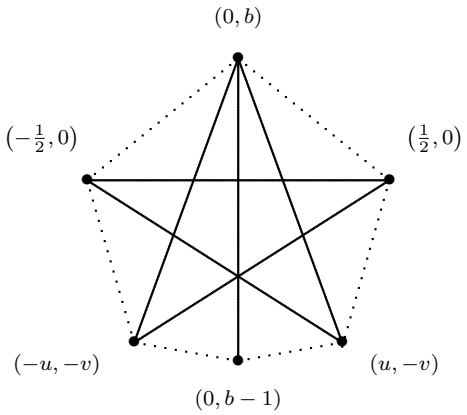

Figure 4: An cycle of length five with a pending diameter

We next apply Proposition 2 in which f_1 is the perimeter P, f_2 is the area A, $g_1(q) = P(q)$ and $g_2(q) = A(q)$. The corresponding optimization problem (5) is

$$
(\mathrm{T}) \left\{
\begin{array}{lll}
\max\limits_{x,y\in\mathbb{R}^6; q\in\mathbb{R}} & \frac{1}{2}\sum\limits_{i=1}^{5}(x_i y_{i+1} - x_{i+1}y_i) & \\
& -\frac{1}{4}\left(\sqrt{q^2-1} + \frac{1}{q}\sqrt{16-q^2} + \frac{1}{q}\sqrt{q^2-1}\sqrt{16-q^2} - \frac{q}{2}\sqrt{16-q^2} - 1\right) & \\
\text{s.t.} & \frac{1}{2}\sum\limits_{i=1}^{5}(x_i y_{i+1} - x_{i+1}y_i) & \\
& -\frac{1}{4}\left(\sqrt{q^2-1} + \frac{1}{q}\sqrt{16-q^2} + \frac{1}{q}\sqrt{q^2-1}\sqrt{16-q^2} - \frac{q}{2}\sqrt{16-q^2} - 1\right) \geq \varepsilon & \text{(T0)} \\
& x_1 + \sum\limits_{i=1}^{5}\|(x_{i+1}, y_{i+1}) - (x_i, y_i)\| - q & \\
& \qquad -\sqrt{6 - \frac{2}{q}\sqrt{q^2-1}\sqrt{16-q^2}} - \sqrt{8 - 2\sqrt{q^2-1} - \frac{2}{q}\sqrt{16-q^2}} \geq \epsilon & \text{(T1)} \\
& \|(x_{i+3}, y_{i+3}) - (x_i, y_i)\|^2 \leq 1 & i \in \{1,2,3\} \quad \text{(T2)} \\
& \|(x_6, y_6) - (x_2, y_2)\|^2 \leq 1 & \text{(T3)} \\
& \|(x_{i+2}, y_{i+2}) - (x_i, y_i)\|^2 \leq 1 & i \in \{1,2,3,4\} \quad \text{(T4)} \\
& \|(x_5, y_5) - (x_1, y_1)\|^2 \leq 1 & \text{(T5)} \\
& x_{i+1}y_i + x_{i+2}y_{i+1} + x_i y_{i+2} \leq x_i y_{i+1} + x_{i+1}y_{i+2} + x_{i+2}y_i & i \in \{1,2,3,4\} \quad \text{(T6)} \\
& \|(x_4, y_4) - (x_3, y_3)\|^2 \leq x_1^2 & \text{(T7)} \\
& \|(x_{i+1}, y_{i+1}) - (x_i, y_i)\|^2 \leq 0.978^2 & i \in \{1,2,4,5\} \quad \text{(T8)} \\
& 0 \leq x_1 \leq 0.978 & \text{(T9)} \\
& -1 \leq x_i \leq 1 & i \in \{2, \cdots, 5\} \quad \text{(T10)} \\
& 0 \leq y_i \leq 1 & i \in \{2, \cdots, 5\} \quad \text{(T11)} \\
& x_6 = y_6 = y_1 = 0 & \text{(T12)} \\
& q \in [1.28356703414671,\ 1.31490238364] & \text{(T13).}
\end{array}
\right.
$$

Constraints (T0–1) are $f_i(x) - g_i(q) \geq \varepsilon$. The constraints (T2–5) ensure that the length of all diagonals (for non-consecutive vertices) is less than or equal to 1. (T6) ensures that the figure is a convex polygon. The constraints (T7–9) use Lemma 1 and impose that the side lengths do not exceed 0.978 and (T7) breaks the symmetry. (T10–11) are trivial bounds and (T12) roots the sixth vertex at the origin and the first one on the positive abscissa. Constraint (T13) is $q \in [\underline{q}, \overline{q}]$.

Bottom part of the Pareto front: A path of length four with a pending diameter

Consider a symmetrical diameter graph composed of a path of length four, together with a pending diameter, and parameterized using the scalar r as illustrated in Figure 5.

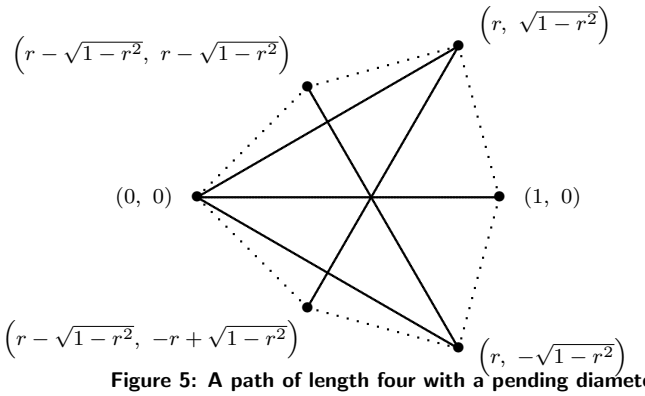

Figure 5: A path of length four with a pending diameter

The perimeter and area of this hexagon can be written as follows

$$\begin{aligned} P(r) &= 2\left(\sqrt{2}(r+\sqrt{1-r}-\sqrt{1-r^2})+\sqrt{5-4r^2-4r\sqrt{1-r^2}}\right), \\ A(r) &= 1+(1-2r)\sqrt{1-r^2}. \end{aligned}$$

The lower bound on r is $\underline{r}=\frac{\sqrt{3}}{2}$ (a lower value would lead to a diagonal of length greater than one). This corresponds to the clipped-Reuleaux hexagon. The upper bound $\overline{r}=0.86935309619661$ corresponds to a hexagon of perimeter $P(\overline{r})=3.100102485+\epsilon$, associated with $\overline{q}$ from the upper part of the Pareto front.

$$(B)\begin{cases} \max\limits_{x,y\in\mathbb{R}^6;r\in\mathbb{R}} & \frac{1}{2}\sum\limits_{i=1}^{5}(x_iy_{i+1}-x_{i+1}y_i)-\left(1+(1-2r)\sqrt{1-r^2}\right) & \\ \text{s.t.} & \frac{1}{2}\sum\limits_{i=1}^{5}(x_iy_{i+1}-x_{i+1}y_i)-\left(1+(1-2r)\sqrt{1-r^2}\right)\geq\varepsilon & \text{(B0)} \\ & x_1+\sum\limits_{i=1}^{5}\|(x_{i+1},y_{i+1})-(x_i,y_i)\| & \\ & \qquad -2\left(\sqrt{2}\left(r+\sqrt{1-r}-\sqrt{1-r^2}\right)+\sqrt{5-4r^2-4r\sqrt{1-r^2}}\right)\geq\varepsilon & \text{(B1)} \\ & \|(x_{i+3},y_{i+3})-(x_i,y_i)\|^2\leq 1 \qquad i\in\{1,2,3\} & \text{(B2)} \\ & \|(x_6,y_6)-(x_2,y_2)\|^2\leq 1 & \text{(B3)} \\ & \|(x_{i+2},y_{i+2})-(x_i,y_i)\|^2\leq 1 \qquad i\in\{1,2,3,4\} & \text{(B4)} \\ & \|(x_5,y_5)-(x_1,y_1)\|^2\leq 1 & \text{(B5)} \\ & x_{i+1}y_i+x_{i+2}y_{i+1}+x_iy_{i+2}\leq x_iy_{i+1}+x_{i+1}y_{i+2}+x_{i+2}y_i \qquad i\in\{1,2,3,4\} & \text{(B6)} \\ & \|(x_4,y_4)-(x_3,y_3)\|^2\leq x_1^2 & \text{(B7)} \\ & \|(x_{i+1},y_{i+1})-(x_i,y_i)\|^2\leq 0.978^2 \qquad i\in\{1,2,4,5\} & \text{(B8)} \\ & 0\leq x_1\leq 0.978 & \text{(B9)} \\ & -1\leq x_i\leq 1 \qquad i\in\{2,3,4\} & \text{(B10)} \\ & -0.978\leq x_5\leq 0.978 & \text{(B11)} \\ & 0\leq y_i\leq 1 \qquad i\in\{3,4\} & \text{(B12)} \\ & 0\leq y_i\leq 0.978 \qquad i\in\{2,5\} & \text{(B13)} \\ & x_6=y_6=y_1=0 & \text{(B14)} \\ & r\in[0.866025403784438,\ 0.86935309619661] & \text{(B15)} \end{cases}$$

Constraints (B0–1) are $f_i(x)-g_i(q)\geq\varepsilon$. The constraints (B2–5) ensure that the length of all diagonals (for non-consecutive vertices) are less than or equal to 1. (B6) ensures that the figure is a convex polygon. The constraints (B7–9) use Lemma 1 and impose that the side lengths do not exceed 0.978 and (B7) breaks the symmetry. (T10–13) are bounds and (B14) roots the sixth vertex at the origin and the first one on the positive abscissa. Constraint (B15) is $r\in[\underline{r},\overline{r}]$.

4 Numerical experiments

Numerical experiments are conducted using an interval global optimization algorithms. The experiments are first conducted on the equilateral hexagon, and then on the non-equilateral hexagon. The latter are decomposed into the top and bottom part of the Pareto front. They are further decomposed to make the experiments tractable.

4.1 IBBA interval global optimization algorithm

IBBA is an interval branch-and-bound based code developed during Messine's and then Ninin's PhD [22, 26, 30]. IBBA is based on interval arithmetic introduced by Moore [28] in 1966 and on a branch-and-bound algorithm in order to solve global optimization problems. The basis of those interval global optimization codes comes from the eighties [31] and these algorithms were strongly improved during the nineties [15, 19, 22]. The originality of IBBA lies mainly in the way to deal with equality and inequality constraints, including constraint propagation techniques [22, 24], and the way to compute bounds by developing reliable linear relaxation techniques based on affine forms and affine arithmetics [18, 23, 27, 30]. Both techniques are now included in recent and efficient global optimization solvers such as COUENNE [10], BARON [33] and IBEX-opt [36]. The global optimization codes based on interval arithmetic have the property to be rigorous and reliable from a numerical point of view; i.e., no floating point operation nor floating point number approximation can provide wrong results. Indeed, all floating point numbers are enclosed in intervals and special care is devoted when floating point operations and approximations are performed. Note that unlike COUENNE and BARON, IBEX-opt and IBBA are *numerically reliable* as defined by Moore in [28]. IBBA was used to design numerous innovative electromechanical actuators [11, 17, 25] and also to solve geometrical problems [5, 16, 30].

Generally, in order to use IBBA or other numerical optimization solvers, it is necessary to slightly relax the equality constraints by a tolerance $\delta > 0$ in order to obtain a numerical solution. Moreover, using IBBA, the numerical solution is proved to be the global one within the tolerance ε fixed by the user. Therefore, if IBBA converges, it is proven that no point (even with real components and not only floating point ones) can be better than the numerical solution (of the relaxed problem) within the fixed tolerance; this also includes all the (real and floating-point) solutions of the original problem. If IBBA terminates without a feasible solution, this means that there is no feasible solution (even real ones) to the problem in which each equality constraint is relaxed by the tolerance δ; this also includes the original problem without relaxing any constraints. Indeed IBBA can guarantee that an optimization problem has strictly no feasible solution.

4.2 The Pareto front for the equilateral small hexagons

Solving problem (E) from of Section 3 using IBBA and with a precision $\varepsilon = 10^{-6}$ for the biobjective functions and with a tolerance of $\delta = 10^{-10}$ on the equality constraints requires 0.46s on a 2.8GHz PC-computer with 10GB to show that there are no feasible solutions. The constraint (E0) is implicitly handled by IBBA as it solves the problem with a precision of ε on the objective function value. This proves that the perimeter P and area A of any unit-diameter equilateral hexagon satisfies

$$A \;\leq\; \frac{\sqrt{3}}{2}\left(1-\left(\frac{P}{6}\right)^2\right)+\varepsilon \qquad \text{with } \varepsilon = 10^{-6}.$$

Therefore, the above certifies the $\varepsilon-$Pareto front of the area vs perimeter of the small equilateral hexagons. This $\varepsilon-$Pareto front is represented by the dotted curve in Figure 7.

4.3 The Pareto front for small hexagons

IBBA fails to solve both problems (T) and (B) efficiently, even if constraints on the objective function are added as in the previous subsection. Hence, we further decompose each of the programs (T)

and (B) into three sub-cases by studying the structures of Pareto optimal solutions. This is described in the following proposition.

Proposition 3 *The diameter graphs of a Pareto optimal hexagon have either* $3, 2$ *or* 1 *main diagonals as diameters, and their possible configurations are illustrated in Figure 6.*

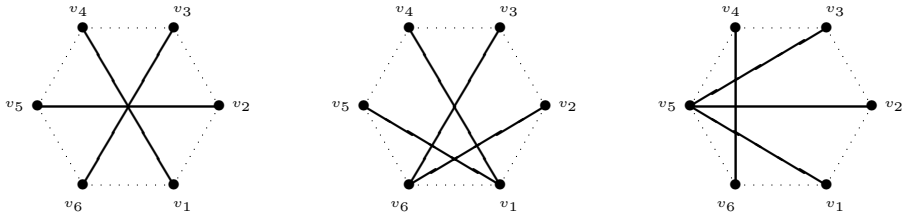

(a) 3 main diagonals (b) 2 main diagonals (c) 1 main diagonal

Figure 6: The three possible diameter graph configurations of Pareto optimal hexagons

Proof. Let $v_1, v_2, \ldots, v_6$ denote the consecutive vertices of a Pareto optimal hexagon. Each vertex is the endpoint of at least one diameter, because moving the vertex away from the center of the hexagon increases both its area and its perimeter. None of the sides are diameters, because Lemma 1 ensures that the side lengths are strictly less than one. Furthermore, any two diameters intersect in the hexagon [7].

We consider four cases involving the three main diagonals of the hexagon.

Case (a): The three main diagonals are diameters. This case trivially corresponds to subfigure (a).

Case (b): Exactly two main diagonals are diameters. Without any loss of generality, suppose that the main diagonals v_1v_4 and v_3v_6 are diameters but v_2v_5 is not a diameter. Since v_2 is the endpoint of a diameter, we may assume that v_2v_6 is a diameter. Finally, v_5 is also the endpoint of the diameter, and its other endpoint is not v_2, and cannot be v_3 (otherwise two diameters would be non-intersecting). The remaining possibility is that v_5v_1 is a diameter, as illustrated in subfigure (b).

Case (c): Only one main diagonal is a diameter. Without any loss of generality, suppose that the main diagonal v_2v_5 is a diameter but v_1v_4 and v_3v_6 are not diameters. We refine the analysis into two more subcases involving the diameter involving v_1.

- v_1v_5 is a diameter. It follows that v_4v_2 cannot be a diameter (otherwise two diameters would be non-intersecting), and consequently v_4v_6 is a diameter. The diagonal v_3v_1 cannot be a diameter, and therefore v_3v_5 is a diameter, as illustrated in subfigure (c).
- v_1v_3 is a diameter. It follows that v_4v_6 cannot be a diameter (otherwise two diameters would not intersect), and consequently, both v_4v_2 and v_4v_2 are diameters. By relabeling the vertices (adding 3 modulo 6), the diameter graph corresponds to subfigure (c).

Case (d): None of the main diagonals are diameters. If none of the main diagonals are diameters, then by symmetry, we can assume that v_4v_6 is a diameter. It follows that v_1v_3 cannot be a diameter (otherwise two diameters would not intersect), and consequently, both v_1v_5 and v_3v_5 are diameters. This leads to an impossibility: v_2 cannot be the endpoint of any diameters.

□

Using Proposition 3 and the two programs (T) and (B), 6 optimization subproblems are generated by just changing some inequality constraints into equality constraints; for example, the constraints (T3) and (B3), for case (b) are both replaced by $\|(x_6, y_6) - (x_2, y_2)\|^2 = 1$.

For each of these six problems, IBBA shows with a tolerance of $\delta = 10^{-10}$ (on the equality constraints) and a precision $\varepsilon = 10^{-6}$ that there is no feasible solution. The constraints (T0) and (B0) are implicitly handled by IBBA as it solves the problem with a precision of ε on the objective function value. The CPU times of these numerical proofs are reported in Table 3. The overall computational time is close to 24 hours. The CPU time required to solve the three different cases share a comparable order of magnitude.

Table 3: CPU-time in h:m:s used by IBBA to prove the $\varepsilon-$Pareto front for the cases from Proposition 3, on a 2.8GHz PC-computer with 10GB, and with a tolerance of 10^{-10} on the equality constraints

Problem	Case (a)	Case (b)	Case (c)	Total
(T)	3:21:15	4:07:04	2:13:03	9:41:23
(B)	4:39:54	5:07:31	4:21:37	14:09:03
Total	8:01:10	9:14:36	6:34:40	23:50:27

Therefore, using IBBA, we prove that the parametrized Pareto fronts provided in Section 3 for small not necessarily equilateral hexagons are $\varepsilon-$optimal with respect to the area and the perimeter with numerical precision $\varepsilon = 10^{-6}$.

The corresponding $\varepsilon-$Pareto front is plotted in Figure 7. The front for the equilateral case is clearly visible, however, only the bottom part of the front is clearly visible for the non-equilateral case. Careful inspection of the figure reveals the top part. For clarity, the bottom part of Figure 8

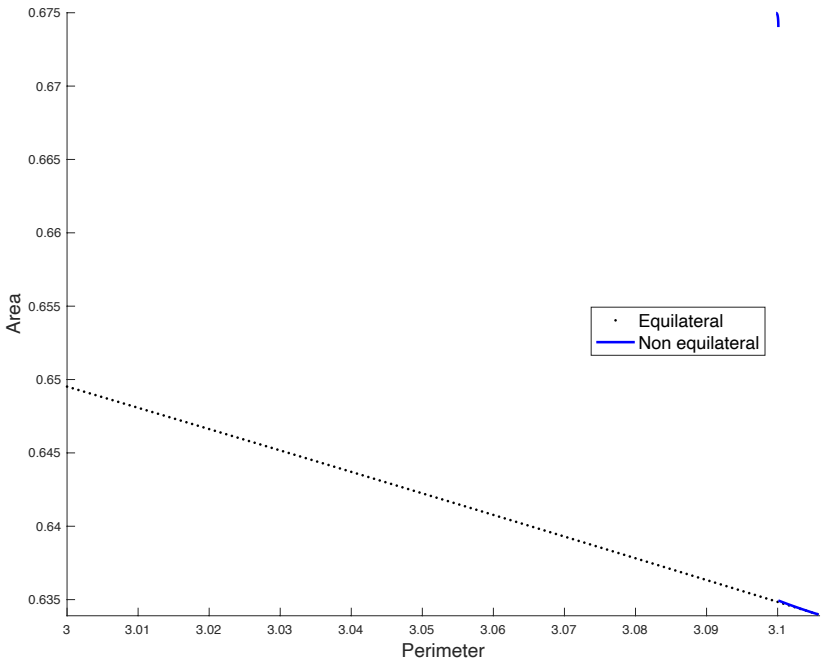

Figure 7: Pareto fronts for the equilateral and non-equilateral hexagons

zooms in on three distinct regions of the fronts. The dotted lines left show the Pareto front of the equilateral hexagon (for small values of the perimeter on the left, and for large values on the right). The full curves of the two graphs on the right show the two disjoint component of the Pareto front of the non-equilateral hexagon.

The top part of Figure 8 depicts the equilateral, the Graham and clipped-Reuleaux hexagons, as well as the two hexagons corresponding to the discontinuity on the Pareto front. All diagonals of length one are also illustrated.

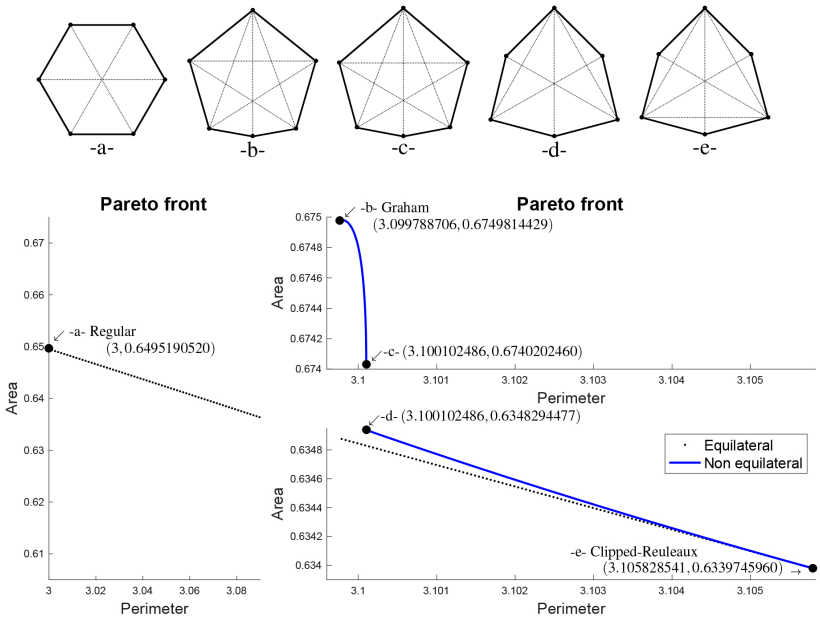

Figure 8: Detailed view of the Pareto fronts for the equilateral and non-equilateral hexagons

5 Discussion

Some numerical experimentations via optimization codes can make it possible to conjecture on the form of a Pareto front. The question of certifying numerically that the conjecture is correct may be formulated as a single-objective optimization problem. Then, by using deterministic global optimization codes, it is possible to prove that these explicit Pareto fronts are optimal within a given threshold ε. This methodology is general and was applied in the present work to the question of finding the Pareto fronts of the area versus perimeter over equilateral small hexagons and over non-equilateral small hexagons.

References

[1] C. Audet. Optimization problems in planar geometry. In S. Cafieri, B. G.-Tóth, E.M.T. Hendrix, L. Liberti, and F. Messine, editors, Proceedings of the Toulouse Global Optimization Workshop, pages 3–6, 2010.

[2] C. Audet. Maximal area of equilateral small polygons. The American Mathematical Monthly, 124(2):175–178, 2017.

[3] C. Audet, J. Bigeon, D. Cartier, S. Le Digabel, and L. Salomon. Performance indicators in multiobjective optimization. Technical Report G-2018-90, Les cahiers du GERAD, 2018.

[4] C. Audet, P. Hansen, and F. Messine. Extremal problems for convex polygons. Journal of Global Optimization, 38(2):163–179, 2007.

[5] C. Audet, P. Hansen, and F. Messine. The small octagon with longest perimeter. Journal of Combinatorial Theory and Applications, Series A, 114(1):135–150, 2007.

[6] C. Audet, P. Hansen, and F. Messine. Extremal Problems for Convex Polygons - An Update. In P.M. Pardalos and T.F. Coleman, editors, Lectures on Global Optimization, volume 55 of Fields Institute Communications, pages 1–16. American Mathematical Society, 2009.

[7] C. Audet, P. Hansen, F. Messine, and S. Perron. The minimum diameter octagon with unit-length sides: Vincze's wife's octagon is suboptimal. Journal of Combinatorial Theory. Series A, 108(1):63–75, 2004.

[8] C. Audet, P. Hansen, F. Messine, and J. Xiong. The largest small octagon. J. Combin. Theory Ser. A, 98(1):46–59, 2002.

[9] C. Audet, P. Hansen, and D. Svrtan. Using symbolic calculations to determine largest small polygons. Technical Report G-2019-57, Les cahiers du GERAD, 2019.

[10] P. Belotti, J. Lee, L. Liberti, F. Margot, and A. Wachter. Branching and bounds tightening techniques for non-convex MINLP. Optimization Methods and Software, 24:597–634, 2009.

[11] B. Nogarède F. Messine and J.L. Lagouanelle. Optimal design of electromechanical actuators: A new method based on global optimization. IEEE Transactions on Magnetics, 34:299–308, 1998.

[12] J. Foster and T. Szabo. Diameter graphs of polygons and the proof of a conjecture of graham. Journal of Combinatorial Theory, Series A, 114(8):1515–1525, 2007.

[13] S. Gashkov. Inequalities for the area and perimeter of a convex polygon. Kwant, 10:15–19, 1985. In Russian: С.Б. Гашков, Неравенства дља плошади и периметра выпуклого многоугольника, Квант, 10, 15–19 (1985).

[14] R.L. Graham. The largest small hexagon. Journal of Combinatorial Theory, Series A, 18:165–170, 1975.

[15] E. Hansen. Global Optimization using Interval Analysis. Marcel Dekker, New York, 1992.

[16] D. Henrion and F. Messine. Finding largest small polygons with GloptiPoly. In S. Cafieri, B.G.-Tóth, E.M.T. Hendrix, L. Liberti, and F. Messine, editors, Proceedings of the Toulouse global optimization workshop), pages 63–66, 2010.

[17] F. Messine J. Fontchastagner and Y. Lefèvre. Design of electrical rotating machines by associating deterministic global optimization algorithm with combinatorial analytical and numerical models. IEEE Transactions on Magnetics, 43:3411–3419, 2007.

[18] F. Messine J. Ninin and P. Hansen. A reliable affine relaxation method for global optimization. 4OR, 13:247–277, 2014.

[19] R. Baker Kearfott. Rigourous Global Search: Continuous Problems. Kluwer Academic Publishers, 1996.

[20] M. Li and X. Yao. Quality evaluation of solution sets in multiobjective optimisation: A survey. ACM Computing Surveys, 52(2):26:1–26:38, 2019.

[21] R.T. Marler and J.S. Arora. Survey of multi-objective optimization methods for engineering. Structural and Multidisciplinary Optimization, 26(6):369–395, 2004.

[22] F. Messine. Méthodes d'optimisation globale basées sur l'analyse d'intervalle pour la résolution des problèmes avec contraintes. PhD thesis, Toulouse-INP, ENSEEIHT-IRIT, University of Toulouse, Toulouse, France, 1997.

[23] F. Messine. Extensions of affine arithmetic: Application to unconstrained global optimization. Journal of Universal Computer Science, 11:992–1015, 2002.

[24] F. Messine. Deterministic global optimization using interval constraint propagation techniques. RAIRO-Operations Research, 38:277–293, 2004.

[25] F. Messine. A deterministic global optimization algorithm for design problems. In G. Savard C. Audet, P. Hansen, editor, Essays and Surveys in Global Optimization, pages 267–294. Springer, 2005.

[26] F. Messine. L'Optimisation Globale par Intervalles : de l'Etude Théorique aux Applications. PhD thesis, Toulouse-INP, ENSEEIHT-IRIT, University of Toulouse, Toulouse, France, 2006.

[27] F. Messine and A. Touhami. A general reliable quadratic form: An extension of affine arithmetic. Reliable Computing, 12:171–192, 2006.

[28] R. E. Moore. Interval Analysis. Prentice-Hall Inc., Englewood Cliffs, 1966.

[29] M.J. Mossinghoff. Isodiametric problems for polygons. Discrete and Computational Geometry, 36:363–379, 2006.

[30] J. Ninin. Optimisation Globale basé sur l'Analyse d'Intervalles: Relaxation affine et limitation de la mémoire. PhD thesis, Toulouse-INP, ENSEEIHT-IRIT, University of Toulouse, Toulouse, France, 2010.

[31] H. Ratschek and J. Rokne. New Computer Methods for Global Optimization. Hellis Horwood Ltd, 1986.

[32] K. Reinhardt. Extremale polygone gegebenen durchmessers. Jahresber. Deutsch. Math. Verein, 31:251–270, 1922.

[33] N.V. Sahinidis. Baron: A general purpose global optimization software package. Journal of Global Optimization, 8(2):201–205, Mar 1996.

[34] S. Shan and G. G. Wang. Survey of modeling and optimization strategies to solve high-dimensional design problems with computationally-expensive black-box functions. Structural and Multidisciplinary Optimization, 41(2):219–241, 2010.

[35] N.K. Tamvakis. On the perimeter and the area of the convex polygon of a given diameter. Bull. Greek Math. Soc., 28:115–132, 1987.

[36] G. Trombettoni, I. Araya, B. Neveu, and G. Chabert. Inner Regions and Interval Linearizations for Global Optimization. In AAAI, pages 99–104, 2011.

[37] S. Vincze. On a geometrical extremum problem. Acta Sci. Math. Szeged, 12:136–142, 1950.

[38] P.L. Yu. Cone convexity, cone extreme points and nondominated solutions in decision problems with multi-objectives. Journal of Optimization Theory and Application, 14:319–377, 1974.

[39] A. Zhou, B.-Y. Qu, H. Li, S.-Z. Zhao, P. N. Suganthan, and Q. Zhang. Multiobjective evolutionary algorithms: A survey of the state of the art. Swarm and Evolutionary Computation, 1(1):32–49, 2011.